J. Fluid Mech. (1971), *vol.* 46, *part* 2, *pp.* 241–265
Printed in Great Britain

Resonant response of harbours: an equivalent-circuit analysis

By JOHN W. MILES†

Institute of Geophysics and Planetary Physics, University of California, La Jolla

(Received 27 April 1970 and in revised form 16 September 1970)

The surface-wave response of a harbour to a prescribed, incident wave is calculated on the hypotheses of shallow-water theory, an ideal fluid, and a narrow mouth, M. An equivalent electrical circuit is constructed, in which the incident-wave displacement in M appears as the input voltage and the flow through M appears as the input current. This circuit contains a *radiation impedance*, Z_M, which comprises resistive and inductive terms, and a *harbour impedance*, Z_H, which comprises an infinite sequence of parallel combinations of inductance and capacitance that bear a one-to-one correspondence with the natural modes of the closed harbour, together with a single capacitor, which corresponds to the degenerate mode of uniform displacement and dominates the response of the harbour as a Helmholtz resonator. Variational approximations to Z_H and Z_M are developed. The equivalent circuit exhibits parallel resonance at the resonant frequencies of the closed harbour, ω_n, and series resonance at a second set of frequencies, $\tilde{\omega}_n$, where $\tilde{\omega}_n \downarrow \omega_n > 0$ and $\tilde{\omega}_0 \downarrow 0$ as $M \rightarrow 0$; $\tilde{\omega}_0$ corresponds to the Helmholtz mode. A narrow canal between the coastline and the harbour is represented by a four-terminal network between Z_M and Z_H. It is shown that narrowing the harbour mouth and/or increasing the length of the canal does not affect the mean response of the harbour to a broad-band, random input except in the Helmholtz mode, but that it does increase significantly the response in that mode, which may dominate tsunami response. The general results are applied to circular and rectangular harbours. The numerical calculation of Z_H for an arbitrarily shaped harbour is discussed.

1. Introduction

We consider (see figure 1) the surface-wave response of a harbour to a prescribed, incident wave in an exterior half-space on the hypotheses of linearized, shallow-water theory, an ideal fluid, and a narrow mouth (see below). The elements of this important engineering problem are reasonably well understood, but the synthesis is complicated in detail (see Miles & Munk 1961; Hwang & Tuck 1970; Carrier, Shaw & Miyata 1970; Lee 1971; Garrett 1970). It therefore appears worthwhile to invoke the equivalent-circuit techniques that have proved so efficient in attacking analogous problems in acoustics and electromagnetic theory. These techniques offer significant advantages in practice: (i) the sub-

† Also Department of Aerospace and Mechanical Engineering Sciences.

problems of external radiation, channel coupling, and internal resonance may be attacked separately; (ii) the equivalent-circuit parameters may be expressed as homogeneous, quadratic forms that may be simply approximated without solving the complete boundary-value problem; (iii) observed values (including those from model experiments) of dominant parameters, such as resonant frequencies, may be incorporated in preference to, or in place of, theoretical values;

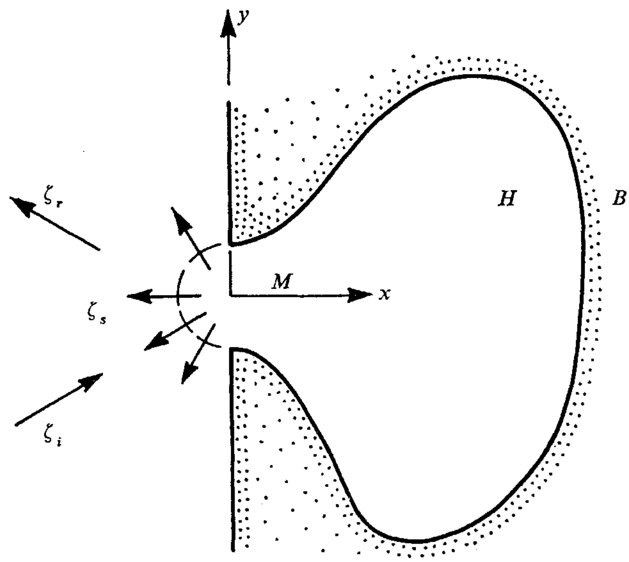

FIGURE 1. Schematic diagram of harbour opening on straight coast line; ζ_i, ζ_r and ζ_s are, respectively, the incident, specularly reflected, and scattered waves.

(iv) empirically determined dissipation parameters (resistances) may be incorporated; (v) analogue computation, both conceptual and electrical, may be invoked to expedite understanding of the resonant response.

Referring to figure 1, we consider a harbour H that opens to the sea through a narrow mouth M in a straight coastline, $x = 0$. Let

$$\zeta_i(x,y) = \tfrac{1}{2}V_i \exp\{-jk(x\cos\theta_i + y\sin\theta_i)\} \tag{1.1}$$

and

$$\zeta_r \equiv \zeta_i(-x,y) \tag{1.2}$$

be the complex amplitudes of the incident and specularly reflected (from $x = 0$) waves on the hypothesis of the monochromatic time dependence $\exp(j\omega t)$, where ζ denotes free-surface displacement (we omit the modifier *complex amplitude of* throughout the subsequent development), k is the wave-number, and

$$V_i \equiv 2\zeta_i(0,0)$$

is a measure of the excitation of the harbour through M. By *narrow*, we imply

$$a/R \ll 1 \quad \text{and} \quad ka \ll 1, \tag{1.3a,b}$$

where a is the width of M, and R is a characteristic dimension of H. These restrictions imply that the motion within H is small, and that the energy of the motion induced by V_i (or, more precisely, by the pressure $\rho g V_i$) is dominantly kinetic and concentrated near M (the narrowness of which implies locally high velocities), except in the spectral neighbourhoods of the resonant frequencies of the harbour. An appropriate measure of this dominant motion is the flow through M, say I, which, by hypothesis (linearized theory), must be simply proportional to V_i. We regard V_i and I as the voltage and current at the input terminals of an equivalent circuit and seek a description of the resonant response of the harbour in terms of the voltages induced in this equivalent circuit.†

The input impedance, $Z_i \equiv V_i/I$, for the configuration of figure 1 may be resolved (see figure 2(*a*)) into a series combination of a radiation impedance, $Z_M \equiv R_M + jX_M$, and a harbour impedance, $Z_H \equiv jX_H$, where $R_M|I|^2$, $X_M|I|^2/\omega$,

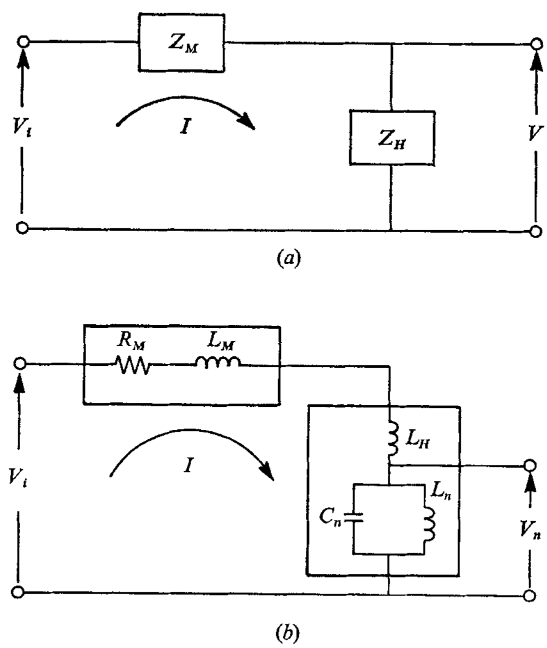

FIGURE 2. Equivalent circuit for harbour opening directly at coastline: (*a*) implied by (3.2); (*b*) implied by (3.2) and (4.5).

and $X_H|I|^2/\omega$ are respectively proportional to the power radiated from H through M (in the form of a scattered wave, ζ_s), the non-radiated energy stored in the exterior half-space, and the energy stored in the harbour (we also could incorporate an empirical, resistive component in Z_H, say R_H, to account for an energy dissipation proportional to $R_H|I|^2$). We infer from the solution of the corresponding acoustical radiation problem (Miles 1948; § 3 below) that both R_M and X_M are bounded, positive-definite functions of ω, by virtue of which we may regard them as single resistive and inductive elements, respectively (although neither R_M nor X_M has the same frequency dependence as its elementary, electrical counterpart). We infer from the analogy with the corresponding

† There are significant advantages in the inverse analogy, in which voltage and current are analogues of flow and pressure, respectively (cf. Miles 1946); however, these advantages are outweighed by other considerations in the present development.

acoustical resonator (Morse 1948, § 23) that Z_H comprises an infinite sequence of parallel combinations of inductance L_n and capacitance C_n, which bear a one-to-one correspondence to the natural modes of the closed harbour and resonate at the corresponding frequencies, $\omega_n \equiv (L_n C_n)^{-\frac{1}{2}}$, together with a single capacitor C_0, which corresponds to the degenerate mode of uniform displacement, for which $\omega_0 \equiv 0$. The solution within H may be expanded in this infinite set of modes, with the root-mean-square displacement and the kinetic and potential energies in the nth mode being proportional to the voltage across C_n and the energies stored in L_n and C_n, respectively. The arguments of the preceding paragraph suggest that the individual modal impedances are important only in the neighbourhoods of their respective resonant frequencies, and hence that Z_H may be approximated in the neighbourhood of $\omega = \omega_n$ by a lumped inductance, say L_H, in series with either C_0 or the single, parallel combination of L_n and C_n, such that the energy in all modes but the nth is proportional to $L_H|I|^2$. The corresponding equivalent circuit is shown in figure 2(*b*) (we give a quantitative derivation of this equivalent circuit in §§ 2 and 3).

The voltage-amplification ratio, $\mathscr{A}_n \propto |V_n/V_i|$, provides a measure of the resonant response in the neighbourhood of $\omega = \omega_n$. The zeroth mode, in which the harbour acts like a Helmholtz resonator, is unique in that the equivalent circuit reduces to a series combination of R_M, $L_M + L_H$, and C_0 and exhibits a simple, series-resonant behaviour with a resonant frequency, say $\tilde{\omega}_0$, that is determined by a balance between the potential energy stored in H, $\frac{1}{2}C_0|V_0|^2$, and the kinetic energy stored in the vicinity of M, $\frac{1}{2}(L_M + L_H)|I|^2$. The results for the rectangular harbour (Miles & Munk 1961) suggest that the sharpness of the Helmholtz resonance is measured by

$$\delta = \{\log(R/a)\}^{-1}, \tag{1.4}$$

and that
$$\tilde{\omega}_0 = O(\delta^{\frac{1}{2}}), \quad \tilde{\mathscr{A}}_0 = O(1/\delta), \quad \text{and} \quad Q_0 = O(1/\delta) \tag{1.5a, b, c}$$

as $a/R \to 0$, where $\tilde{\mathscr{A}}_n$ is the peak value of $\mathscr{A}_n$, and Q_n is the ratio of the resonant frequency to the half-power bandwidth of the resonance curve for the nth mode.

The resonant response of the harbour in the higher modes is strikingly different from that of a simple, series-resonant circuit in consequence of the proximity of the parallel-resonant frequency, ω_n, at which $Z_i = \infty$, and the series-resonant frequency, $\tilde{\omega}_n$, at which $|Z_i|$ has a minimum and $\mathscr{A}_n = \tilde{\mathscr{A}}_n \gg 1$. We show in § 4 that

$$\tilde{\omega}_n = \omega_n + O(\delta), \quad \tilde{\mathscr{A}}_n = O(1/\delta), \quad \text{and} \quad Q_n = O(1/\delta^2) \quad (n \neq 0). \tag{1.6a, b, c}$$

It follows from (1.5) and (1.6) that narrowing the harbour mouth does not affect the mean-square response to a random excitation in the spectral neighbourhood of $\omega = \omega_n$ (which response is proportional to $\tilde{\omega}_n \tilde{\mathscr{A}}_n^2/Q_n$ if the bandwidth of the random input is large compared with $\delta\omega_n$) except in the Helmholtz mode, but that the response in that mode increases inversely as $\delta^{\frac{1}{2}}$. Miles & Munk (1961) overlooked the proximity of parallel and series resonance in the higher modes and arrived at the erroneous conclusion that narrowing the harbour mouth would increase $\tilde{\omega}_n \tilde{\mathscr{A}}_n^2/Q_n$ for all modes, rather than only the Helmholtz mode, and designated the phenomenon as 'the harbour paradox'. In fact, as pointed out by Garrett (1970), this qualitative conclusion is inconsistent with their quantitative results, which actually imply (1.6) for the higher modes in a narrow rectangular harbour. Garrett also showed that $\tilde{\omega}_n \tilde{\mathscr{A}}_n^2/Q_n$ is similarly invariant for excitation of a circular harbour through an open bottom and correctly conjectured that the result holds generally for the higher modes in any harbour. In brief, the harbour paradox originally stated by Miles & Munk holds only for the Helmholtz mode and otherwise must be replaced by the weaker paradox, that narrowing the harbour mouth has no significant effect on the mean-square response of the higher modes to a random input in the absence of friction (narrowing the mouth increases friction, thereby decreasing the response, in a real harbour). It follows that the higher modes are not likely to be strongly excited, but that the Helmholtz mode may dominate the response of a narrow-mouthed harbour to an exterior disturbance that has significant energy in the spectral neighbourhood of $\tilde{\omega}_0$.

Carrier, Shaw & Miyata (1970) consider a harbour that communicates with the coast through a narrow canal and find that both $\tilde{\mathscr{A}}_0$ and Q_0 are significantly increased (as might be inferred from the analogy with the classical Helmholtz resonator; cf. Rayleigh 1945, § 307). We show in § 5 that such a canal is analogous to an electrical transmission line and may be replaced by a symmetrical, four-terminal network for the calculation of V_n (see figure 6). The analogy with the transmission line rests on the hypothesis that only plane waves are excited in the canal. We examine the effects of higher modes in the appendix and show that the elements of the four-terminal network may be appropriately generalized, but that the plane-wave approximation is likely to be adequate if the breadth of the channel is less than a half-wavelength.

The precise determination of Z_M and Z_H requires the solution of an integral equation for the normal velocity in M (or, in the case of an intervening canal, a pair of integral equations for the normal velocities across the terminal sections of the canal). The formulation of §§ 2 and 3 yields variational approximations to Z_M and Z_H that are invariant under a scale transformation (i.e a change in the mean value) of the velocity in M and stationary with respect to first-order variations of this velocity about the true solution to the integral equation (cf. Miles & Munk (1961) and Miles (1946, 1948, 1967); we omit the explicit formulation of the integral equation and further discussion of the variational principle in the present development). The resulting representation of Z_M is relatively insensitive to the geometry of H and yields a simple, explicit approximation that depends essentially only on ka. The corresponding representation of Z_H requires Green's function (subject to a Neumann boundary condition) for the closed harbour, the explicit, analytical construction of which is possible only for those boundaries (rectangular, circular or circular-sector, and elliptic or elliptic-hyperbolic sector) that permit separation of variables; however, we may infer the matrix representation of this Green's function for a polygonal approximation to an arbitrarily shaped harbour from Lee's (1971) collocation solution of the general problem. We give numerical results for circular and rectangular harbours in §§ 6 and 7, with special emphasis on the Helmholtz mode. It appears from these results that a large harbour with a short entrance or a small harbour with an entry canal of length comparable with R may resonate in the Helmholtz mode under tsunami excitation.

2. Harbour impedance

We now give a quantitative derivation of Z_H on the aforementioned hypotheses of linearized, shallow-water theory and monochromatic time dependence. Let x and y be the Cartesian co-ordinates in the free surface, t the time, ω the angular frequency, h the depth,

$$c = (gh)^{\frac{1}{2}} \quad \text{and} \quad k = \omega/c \tag{2.1a,b}$$

the wave speed and wave-number, $\hat{\zeta}$ the free-surface displacement, $\hat{u}$ the x-component of the particle velocity, ζ and u the corresponding complex amplitudes, such that

$$\{\hat{\zeta}(x,y,t), \hat{u}(x,y,t)\} = \mathscr{R}[\{\zeta(x,y), u(x,y)\}\, e^{j\omega t}], \tag{2.2}$$

where $\mathscr{R}$ implies *the real part of* and $j \equiv \sqrt{-1}$,

$$I = \int_M u\, dS \quad (dS = h\, dy) \tag{2.3}$$

the flow through M,

$$V = \left(\int_M u^*\, dy\right)^{-1} \int_M \zeta u^*\, dy \tag{2.4}$$

a weighted measure of the displacement in M, where u^* is the complex conjugate of u,

$$Z_H \equiv V/I = h^{-1} \left|\int_M u\, dy\right|^{-2} \int_M \zeta u^*\, dy \tag{2.5}$$

the *harbour impedance*, and

$$P = \tfrac{1}{2}\mathscr{R}\left\{\rho g h \int_M \zeta u^*\, dy\right\} = \tfrac{1}{2}\rho g \mathscr{R}(VI^*) \tag{2.6}$$

the rate at which energy flows through M. We may regard αV, βI, $(\alpha/\beta)\, Z_H$, and $\alpha\beta\mathscr{R}(VI^*)$ as the voltage, current, impedance, and power in an equivalent electrical circuit, where the constants of proportionality, α and β, may be chosen to obtain convenient electrical units. The choice $\alpha = \beta = 1$ is implicit in the discussion of § 1, but not in what follows except as noted.

The shallow-water equations for ζ and u are (Lamb 1932, § 189; Lamb uses $i\sigma$ where we use $j\omega$)

$$(\nabla^2 + k^2)\, \zeta = 0 \quad (\nabla^2 \equiv \partial^2/\partial x^2 + \partial^2/\partial y^2), \tag{2.7a}$$

and

$$u = (jg/\omega)\, (\partial\zeta/\partial x). \tag{2.7b}$$

The solution of (2.7) for an assumed velocity in M, subject to the boundary condition that the normal derivative of ζ, $\mathbf{n} \,.\, \nabla\zeta$, vanish on B, the lateral boundary of the free surface in H, is given by (Sommerfeld 1949, §§ 10 and 27)

$$\zeta(x,y) = (j\omega/g) \int_M G(x,y;0,\eta)\, u(0,\eta)\, d\eta, \tag{2.8}$$

where

$$G(x,y;\xi,\eta) = \sum_n (k_n^2 - k^2)^{-1}\, \psi_n(x,y)\, \psi_n(\xi,\eta) \tag{2.9}$$

is the point-source Green's function for H, the ψ_n are the normalized eigenfunctions for the closed harbour, and the summation is over the complete set of these functions. The ψ_n are real and satisfy

$$(\nabla^2 + k_n^2)\,\psi_n = 0 \quad (x, y \text{ in } H), \tag{2.10a}$$

$$(\mathbf{n}.\nabla)\,\psi_n = 0 \quad \text{on} \quad B, \tag{2.10b}$$

and

$$\int_H \psi_m \psi_n \, dA = \delta_{mn}, \tag{2.10c}$$

where k_n are the eigenvalues (resonant wave-numbers), and δ_{mn} is the Kronecker delta. We designate the degenerate (but non-trivial) solution corresponding to $\psi = \text{const.}$ by $n = 0$:

$$k_0 = 0, \quad \psi_0 = A^{-\frac{1}{2}}, \tag{2.11}$$

where A is the area of H. We also note that more explicit results may require the use of two indices to count off the individual modes.

The exact determination of the assumed velocity, $u(0, y)$, requires u and ζ to be matched across M to the corresponding solution of the exterior boundary-value problem (see § 3 below). This matching condition yields an integral equation for $u(0, y)$, the exact solution of which in finite terms does not appear to be possible; however, simple approximations to $u(0, y)$ are capable of yielding excellent approximations to Z_M and Z_H by virtue of the associated variational principle (cf. Miles 1946, 1948, 1967; Miles & Munk 1961). We proceed directly to such approximations by introducing the normalized trial function $f(y)$, such that

$$u(0, y) = (I/h)\,f(y), \quad \int_M f(y)\,dy = 1. \tag{2.12a, b}$$

In the subsequent development, we neglect the dependence of $f(y)$ on κ and assume that it depends only on the geometry of M; see, e.g. (3.5) and (3.6) below. The validity of this approximation, which also implies that $f(y)$ is real, depends essentially on the antecedent approximation $ka \ll 1$.

Substituting (2.12) into (2.4) and (2.8) and combining the results in (2.5), we obtain

$$V = \int_M \zeta f^* \, dy \tag{2.13}$$

and

$$Z_H = (j\omega/c^2) \int_M \int_M G(0, y; 0, \eta)\, f^*(y)\, f(\eta)\, d\eta\, dy. \tag{2.14}$$

Substituting (2.9) into (2.14), we obtain

$$Z_H = \sum_n Z_n, \tag{2.15}$$

where

$$Z_n = j\omega(\omega_n^2 - \omega^2)^{-1} \left| \int_M \psi_n f \, dy \right|^2 \tag{2.16a}$$

$$= (j\omega/c^2)\,\mu_n(\kappa_n - \kappa)^{-1} \tag{2.16b}$$

is the *modal impedance* (note that $Z_0 = 1/j\omega A$),

$$\mu_n = A \left| \int_M \psi_n f \, dy \right|^2 \tag{2.17}$$

is a dimensionless measure of the excitation of the nth mode through M (note that $\mu_0 \equiv 1$), and

$$\kappa \equiv k^2 A = \omega^2(A/gh) \quad \text{and} \quad \kappa_n \equiv k_n^2 A = \omega_n^2(A/gh) \tag{2.18a,b}$$

are dimensionless measures of (the square of) the frequency and of the eigenvalue k_n^2. The Z_n in the equivalent circuit appear in series, Z_0 appears as a capacitor, and each of the remaining Z_n appears as a parallel combination of an inductor and capacitor, with inductance and capacitance proportional to $\mu_n/(\kappa_n c^2)$ and A/μ_n, respectively, that exhibits parallel resonance at $\omega = \omega_n = k_n c$. The equivalent-circuit parameters in § 1 are $L_n = \mu_n/(\kappa_n c^2)$ and $C_n = A/\mu_n$.

The dominant terms in Z_H as $\kappa \to 0$ are Z_0 and the sum of the inductive reactances obtained by neglecting κ relative to κ_n in the remaining Z_n. Let

$$G^{(0)}(y,\eta) \equiv \lim_{k\to 0}[G(0,y;0,\eta)+\kappa^{-1}] \tag{2.19a}$$

$$= \sum_n{}' k_n^{-2}\psi_n(0,y)\,\psi_n(0,\eta) \tag{2.19b}$$

and

$$\Lambda_H^{(0)} \equiv \int_M\int_M G^{(0)}(y,\eta)f^*(y)f(\eta)\,d\eta\,dy \tag{2.20a}$$

$$= \sum_n{}' \mu_n\kappa_n^{-1}, \tag{2.20b}$$

where the prime implies the exclusion of $n = 0$ from the summations; then

$$Z_H = (j\omega/c^2)\,[\Lambda_H^{(0)} - \kappa^{-1} + \sum_n{}' \mu_n(\kappa/\kappa_n)\,(\kappa_n-\kappa)^{-1}], \tag{2.21}$$

where $\Lambda_H^{(0)}$ is independent of κ and depends only on the geometry of the harbour by virtue of the corresponding approximation for $f(y)$.

The representation (2.9) for the Green's function is ideally suited to the representation of Z_H in terms of modal impedances, but the analytical determination of the eigenfunctions is feasible only for those shapes that permit the solution of the Helmholtz equation by separation of variables. An alternative determination of $G(x,y;0,\eta)$ is provided by (cf. Miles & Munk 1961)

$$(\nabla^2+k^2)\,G = 0 \quad (x,y \text{ in } H), \tag{2.22a}$$

$$(\mathbf{n}\,.\,\nabla)\,G = 0 \quad (x,y \text{ on } B), \tag{2.22b}$$

and

$$\partial G/\partial x = -\delta(y-\eta) \quad (x,y \text{ in } M). \tag{2.22c}$$

Applying Green's second theorem to $G(x,y;0,\eta)$ and the fundamental solution $-\tfrac{1}{2}jH_0^{(1)}(k|\mathbf{r}-\mathbf{r}_1|)$, where $\mathbf{r}$ and $\mathbf{r}_1$ are points in H and on $B+M$, respectively, we may transform (2.22) to an integral equation which is equivalent to that formulated by Lee (1971).† Dividing B into N, and M into p, segments of length Δ and replacing $G(0,y;0,\eta)$ by a $p\times p$ matrix with its elements evaluated at the corresponding points in M, say $\mathbf{G}$, we obtain

$$\mathbf{G} = \Delta^{-1}\mathbf{M}_p, \tag{2.23}$$

† Lee assumes the time dependence $\exp(-i\omega t)$, in consequence of which it might appear necessary to replace $-iH_0^{(1)}$ in his formulation by $jH_0^{(2)}$ in the present formulation; in fact this is unnecessary by virtue of the fact that G is real (since there is no dissipation in the harbour). The essential requirement is that the fundamental solution satisfy the Helmholtz equation and be singular like $(1/\pi)\log|\mathbf{r}-\mathbf{r}_1|$ as $\mathbf{r}\to\mathbf{r}_1$.

where $\mathbf{M}_p$ is Lee's $p \times p$, truncated matrix, with the element at i and j in his notation corresponding to the element at $(0, y)$ and $(0, \eta)$ in the present notation. Representing $f(y)$ by a column matrix of order p, say $\mathbf{f}$, subject to the constraint that the sum of its elements be equal to $1/\Delta$, and invoking (2.14), we obtain

$$Z_H = (j\omega/c^2)\,\Delta\mathbf{f}^*\mathbf{M}_p\mathbf{f}, \tag{2.24}$$

where $\mathbf{f}^*$ is the complex-conjugate of the transpose of $\mathbf{f}$ (i.e. a row matrix made up of the complex conjugates of the elements of $\mathbf{f}$). We remark that $\mathbf{M}$ is Hermitian by virtue of which $\mathbf{f}^*\mathbf{M}\mathbf{f}$ (a Hermitian form) is real.

(Hwang & Tuck (1970) also develop a numerical method for the treatment of arbitrarily shaped harbours; however, they do not distinguish between the exterior and interior of H, in consequence of which their treatment is less convenient than that of Lee in the present context.)

3. Radiation impedance

The solution of the shallow-water equations (2.7) in the exterior half-space $(x < 0)$ for a prescribed incident wave, say $\zeta_i(x, y)$, and the assumed velocity $u(0, y)$ in the harbour mouth is given by (Miles & Munk 1961)

$$\zeta(x,y) = \zeta_i(x,y) + \zeta_i(-x,y) + \zeta_s(x,y), \tag{3.1a}$$

where $$\zeta_s(x,y) = -\tfrac{1}{2}(\omega/g)\int_M H_0^{(2)}[k(x^2+|y-\eta|^2)^{\frac{1}{2}}]\,u(0,\eta)\,d\eta \quad (x \leqslant 0), \tag{3.1b}$$

$H_0^{(2)}$ is a Hankel function, the first two terms on the right-hand side of (3.1*a*) give the solution for total reflexion from the plane $x = 0$ (as would occur if M were closed), and ζ_s is the scattered wave. Substituting u into (3.1) from (2.12), setting $x = 0$, and then substituting the result into (2.13), we obtain

$$V = V_i - Z_M I, \tag{3.2}$$

where $$V_i = 2\int_M \zeta_i f^*\,dy \tag{3.3a}$$

$$\doteqdot 2\zeta_1(0,0) \quad (ka \ll 1) \tag{3.3b†}$$

is the *equivalent exciting voltage* of the incident wave, and

$$Z_M = \tfrac{1}{2}(\omega/c^2)\int_M\int_M H_0^{(2)}(k|y-\eta|)\,f^*(y)\,f(\eta)\,d\eta\,dy \tag{3.4}$$

is the *radiation impedance* of the harbour mouth. The equivalent circuit corresponding to (3.2) is sketched in figure 2(*a*).

The following estimates of the velocity-distribution function are suggested by Rayleigh's (1945, § 307) arguments for the (acoustical) Helmholtz-resonator problem:

$$f^{(1)}(y) = 1/a \tag{3.5}$$

and $$f^{(2)}(y) = \pi^{-1}[(\tfrac{1}{2}a)^2 - y^2]^{-\frac{1}{2}} \quad (|y| < \tfrac{1}{2}a). \tag{3.6}$$

† The definition of V_i implicit in (1.1) corresponds to the approximation (3.3*b*).

The distribution $f^{(1)}$ would be realized if a rigid, massless piston were fitted to M, whereas $f^{(2)}$ would be realized in a two-dimensional, potential flow through the corresponding opening in a plane barrier.

Substituting (3.5) and (3.6) into (3.4) and invoking $ka \ll 1$, we place the resulting approximations to Z_M in the form,

$$Z_M = (\omega/c^2)\,[\tfrac{1}{2} + j\Lambda_M(ka)] \quad (ka \ll 1), \tag{3.7}$$

where

$$\pi\Lambda_M^{(1)} = \tfrac{3}{2} - \ln(\tfrac{1}{2}\gamma ka), \tag{3.8}$$

$$\pi\Lambda_M^{(2)} = -\ln(\tfrac{1}{8}\gamma ka), \tag{3.9}$$

and $\ln\gamma = 0{\cdot}577\ldots$ is Euler's constant. The difference between $\Lambda_M^{(1)}$ and $\Lambda_M^{(2)}$ is only 0·036, which illustrates the relative insensitivity of Z_M to the choice of the normalized trial function (by virtue of the implicit variational principle; cf. Miles 1948).

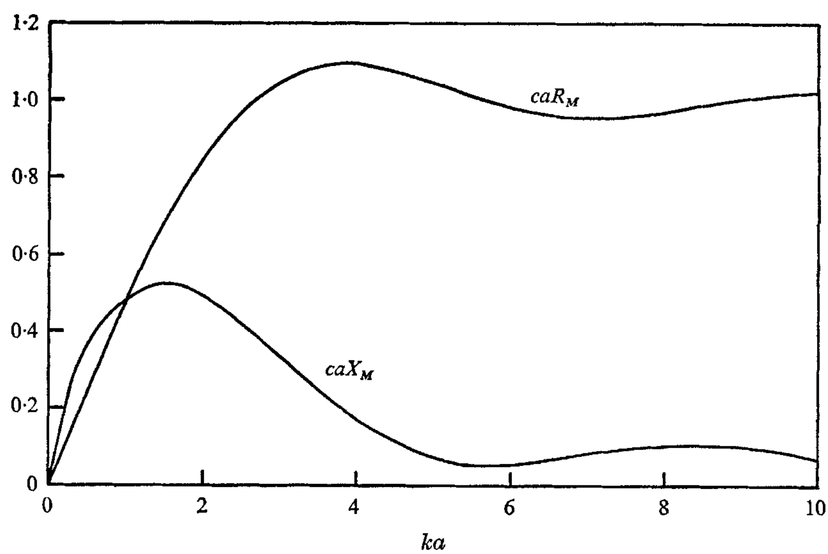

FIGURE 3. The radiation impedance for the harbour mouth, as given by (3.10).

The approximation implied by (3.5) for arbitrary ka is (Miles 1948)

$$caZ_M^{(1)} = \int_0^{ka} H_0^{(2)}(x)\,dx - H_1^{(2)}(ka) + 2j(\pi ka)^{-1} \tag{3.10a}$$

$$\sim 1 + 2j(\pi ka)^{-1} + O\{(ka)^{-\frac{3}{2}}\}, \tag{3.10b}$$

and is plotted in figure 3. The approximation of (3.7) and (3.8) is within 2% of (3.10a) for $ka \leqslant 1$.

The scattered wave implied by (2.12) and (3.1b) at a sufficient distance from the mouth is given by

$$\zeta_s(x, y) = -\tfrac{1}{2}(\omega/c^2)\,IH_0^{(2)}(kr) \quad (ka \ll 1, r \gg a), \tag{3.11}$$

where r is the polar radius measured from the mid-point of M.

4. Resonant response

An appropriate measure of the response of the harbour to a prescribed incident wave is the mean-square elevation, say σ^2, as determined by averaging over both space and time (the temporal average of ζ^2 is $\frac{1}{2}|\zeta|^2$):

$$\sigma^2 = \tfrac{1}{2}A^{-1}\int_H |\zeta|^2 dA. \tag{4.1}$$

Substituting ζ into (4.1) from (2.8), invoking (2.9) for G and (2.12) for u, carrying out the integration over A with the aid of (2.10c), and invoking (2.16b) for $Z_n = V_n/I$, where V_n is the voltage induced across Z_n by I, and (2.17) for μ_n, we obtain

$$\sigma^2 = \tfrac{1}{2}\sum_n \mu_n^{-1}|V_n|^2 \equiv \tfrac{1}{2}|V_i|^2\sum_n \mathscr{A}_n^2(\kappa), \tag{4.2}$$

where

$$\mathscr{A}_n(\kappa) \equiv \mu_n^{-\frac{1}{2}}|V_n/V_i| \tag{4.3a}$$

$$= \mu_n^{-\frac{1}{2}}|Z_n/(Z_M+Z_H)| \tag{4.3b}$$

is the *amplification factor* for the nth mode. Invoking (3.3b) on the hypothesis $a^2/A \ll 1$, we obtain $\sigma_i^2 = \frac{1}{2}|V_i|^2$ for the (temporal) mean-square elevation of $2\zeta_i$, by virtue of which (4.2) reduces to

$$\sigma^2 = \sigma_i^2\sum_n \mathscr{A}_n^2(\kappa). \tag{4.4}$$

The hypotheses (1.3a) and (1.3b) imply $\Lambda_H^{(0)} \gg 1$ and $\Lambda_M \gg 1$, respectively, in consequence of which $|Z_n| \ll |Z_M+Z_H|$ except in the neighbourhood of $\kappa = \kappa_n$. Approximating (2.21) by

$$Z_H \doteqdot (j\omega/c^2)\,[\Lambda_H^{(n)} + \mu_n(\kappa_n-\kappa)^{-1}], \tag{4.5}$$

in this neighbourhood and invoking (2.16b) and (3.7) for Z_n and Z_M, we obtain

$$\mathscr{A}_0(\kappa) = \{\tfrac{1}{4}\kappa^2 + [\kappa\Lambda_0(\kappa)-1]^2\}^{-\frac{1}{2}}, \tag{4.6a}$$

and

$$\mathscr{A}_n(\kappa) = \mu_n^{\frac{1}{2}}\{\tfrac{1}{4}(\kappa-\kappa_n)^2 + [(\kappa-\kappa_n)\,\Lambda_n - \mu_n]^2\}^{-\frac{1}{2}}, \tag{4.6b}$$

where

$$\Lambda_0(\kappa) = \Lambda_H^{(0)} + \Lambda_M(ka), \tag{4.7a}$$

$$\Lambda_n = A_H^{(n)} + \Lambda_M(k_n a) \quad (n \neq 0), \tag{4.7b}$$

and

$$\Lambda_H^{(n)} = \Lambda_H^{(0)} - (\mu_n+1)\,\kappa_n^{-1} + \kappa_n\sum_m{}' \mu_m\kappa_m^{-1}(\kappa_m-\kappa_n)^{-1}, \tag{4.8a}$$

$$\doteqdot \Lambda_H^{(0)}. \tag{4.8b}$$

Both $m = 0$ and $m = n$ are excluded from the summation in (4.8a), which neglects terms of $O(\kappa-\kappa_n)$ as $\kappa \to \kappa_n$, whilst (4.8b) neglects terms of $O(1)$ relative to the logarithmic terms in $\Lambda_H^{(0)}$ and Λ_M as a/R and $ka \to 0$. We assume $\Lambda_n \gg 1$ throughout the subsequent development ($\delta \sim 1/\Lambda_n$ in § 1).

The resonance curves of (4.6a) and (4.6b) are illustrated in figures 10 and 12, using the results derived in § 6 for a circular harbour.

The peak value of $\mathscr{A}_n$, say $\tilde{\mathscr{A}}_n$, occurs at the series-resonant point, say $\kappa = \tilde{\kappa}_n$, where

$$\tilde{\kappa}_0\Lambda_0(\tilde{\kappa}_0) = 1, \tag{4.9a}$$

$$\tilde{\kappa}_n = \kappa_n + \mu_n\Lambda_n^{-1} \quad (n \neq 0), \tag{4.9b}$$

$$\tilde{\mathscr{A}}_0 = 2\tilde{\kappa}_0^{-1}, \tag{4.10a}$$

and

$$\tilde{\mathscr{A}}_n = 2\mu_n^{-\frac{1}{2}}\Lambda_n \quad (n \neq 0). \tag{4.10b}$$

The amplification factor drops off sharply on both sides of $\kappa = \tilde{\kappa}_n$, passes through the points

$$\mathscr{A}(\kappa_n) = \mathscr{A}(2\tilde{\kappa}_n - \kappa_n) = \mu_n^{-\frac{1}{2}}, \tag{4.11}$$

and is $O(1/\Lambda_n)$ for $|\kappa - \kappa_n| \gg 1/\Lambda_n$. The points $\kappa = \kappa_n$ corresponds to parallel resonance ($Z_n = \infty$), for which the total flow through M vanishes ($I = 0$) whilst σ^2 remains of the same order as σ_i^2. We define the Q of the resonant response near $\kappa = \tilde{\kappa}_n$ as the ratio of the resonant frequency to the half-power bandwidth, such that (the frequencies at the half-power points are proportional to $\tilde{\kappa}_n^{\frac{1}{2}}(1 \pm \frac{1}{2}Q_n^{-1})$)

$$\mathscr{A}[\tilde{\kappa}_n(1 \pm Q_n^{-1})] = 2^{-\frac{1}{2}}\tilde{\mathscr{A}}_n. \tag{4.12}$$

Substituting (4.6) into (4.12) and invoking (4.9), we obtain the first approximations

$$Q_0 = 2\tilde{\kappa}_0^{-1} = \tilde{\mathscr{A}}_0 \tag{4.13a}$$

and

$$Q_n = 2\mu_n^{-1}\kappa_n\Lambda_n^2 = \tfrac{1}{2}\tilde{\kappa}_n\mathscr{A}_n^2. \tag{4.13b}$$

Now suppose that the incident wave is random with the power spectral density $S_i(f)$, such that

$$\sigma_i^2 = \int_0^\infty S_i(f)\,df \quad (\omega = 2\pi f), \tag{4.14}$$

where f is the frequency. Generalizing (4.4), we obtain

$$\sigma^2 = \sum_n \int_0^\infty S_i(f)\,|\mathscr{A}_n(\kappa)|^2\,df \tag{4.15}$$

for the power spectral density in the harbour. Substituting (4.6) into (4.15), invoking $\omega = c\kappa/\sqrt{A}$, and calculating the contribution of the resonant peaks at $\omega = \omega_n$ on the hypothesis that their bandwidths are small compared with those of $S_i(f)$, we obtain

$$\sigma^2 = (gh/A)^{\frac{1}{2}} \sum_n \mathscr{P}_n S_i(\tilde{f}_n), \tag{4.16}$$

where

$$\mathscr{P}_n = (4\pi)^{-1}\tilde{\kappa}_n^{-\frac{1}{2}}\tilde{\mathscr{A}}_n^2 \int_0^\infty [1 + (Q_n/\tilde{\kappa}_n)^2(\kappa - \tilde{\kappa}_n)^2]^{-1}\,d\kappa \tag{4.17a}$$

$$\sim \tfrac{1}{4}\tilde{\kappa}_n^{\frac{1}{2}}Q_n^{-1}\tilde{\mathscr{A}}_n^2 \quad (Q_n/\tilde{\kappa}_n \to \infty) \tag{4.17b}$$

is the *power-spectrum-amplification factor* for the nth mode. Substituting (4.9), (4.10) and (4.13) into (4.17*b*), we obtain

$$\mathscr{P}_n = \tfrac{1}{2}\tilde{\kappa}_n^{-\frac{1}{2}}, \tag{4.18}$$

from which we infer that narrowing the harbour mouth does not affect significantly the mean response to a random input except in the Helmholtz mode, but that it does increase significantly the response in that mode (this conclusion ignores the increase in viscous dissipation that would be associated with narrowing the mouth).

The approximation (4.5) is inadequate for closely spaced eigenvalues (near degeneracies). Let κ_m and κ_n ($\kappa_m > \kappa_n$) be adjacent eigenvalues; incorporating the contributions of both of the corresponding terms in the series of (2.21) and assuming $\Lambda_H^{(0)} \gg 1$, as in the approximation (4.8*b*), we obtain

$$Z_H = (j\omega/c^2)\,[\Lambda_H^{(0)} + \mu_m(\kappa/\kappa_m)(\kappa_m - \kappa)^{-1} + \mu_n(\kappa/\kappa_n)(\kappa_n - \kappa)^{-1}], \tag{4.19}$$

in which the last term must be replaced by $-1/\kappa$ if $n = 0$. An appropriate measure of the coupling between the two modes is

$$\epsilon = (\mu_m + \mu_n)^{-1} \Lambda_n (\kappa_m - \kappa_n). \tag{4.20}$$

If $\epsilon \gg 1$, the principal effect of replacing (4.5) by (4.19) in the calculation of resonant response is to increase $\tilde{\kappa}_m$ and decrease $\tilde{\kappa}_n$ by increments of $O(1/\epsilon^2)$; we give an example in § 6 below. If $\epsilon \sim 1$ the resonant peaks of $\mathscr{A}_m(\kappa)$ and $\mathscr{A}_n(\kappa)$ tend to merge, and $\mathscr{A}_m^2(\kappa) + \mathscr{A}_n^2(\kappa)$ exhibits a relatively broad, double-humped peak. If $\epsilon \ll 1$, the two resonant peaks merge and yield the peak value

$$(\mathscr{A}_m^2 + \mathscr{A}_n^2)_{\max} = 4(\mu_m + \mu_n)^{-1} \Lambda_n^2 \quad (n \neq 0) \tag{4.21a}$$

at

$$\kappa = \tilde{\kappa}(\mu_m + \mu_n)^{-1} (\mu_m \kappa_m + \mu_n \kappa_n) + (\mu_m + \mu_n) \Lambda_n^{-1} \tag{4.21b}$$

within $1 + O(\epsilon^2, 1/\Lambda_n)$. If $\kappa_m = \kappa_n$ $(\epsilon = 0)$, the shape of the resonance curve for σ^2 near $\kappa = \kappa_n$ is similar to that for an isolated mode near $\kappa = \kappa_n$, with both peak value and Q reduced in the ratio $\mu_n/(\mu_m + \mu_n)$. The power-spectrum-amplification factor is unchanged.

Turning to the scattered wave, as given by (3.11), we infer from the preceding discussion that ζ_s vanishes at the parallel-resonant frequencies and attains its peak value at the series-resonant frequencies, where $Z_M + Z_H$ reduces to $\frac{1}{2}(\omega/c^2)$; substituting the corresponding value of I into (3.11), we obtain (the peak value)

$$\tilde{\zeta}_s = -V_i H_0^{(2)}(kr) \quad (\omega = \tilde{\omega}_n, ka \ll 1, r \gg a). \tag{4.22}$$

The ratio

$$|\zeta_s/\tilde{\zeta}_s| = \tfrac{1}{2}(\omega/c^2)\, |Z_M + Z_H|^{-1} \tag{4.23a}$$

$$\doteqdot [1 + 4\{\Lambda_n + \mu_n(\kappa_n - \kappa)^{-1}\}^2]^{-\frac{1}{2}} \tag{4.23b}$$

is plotted in figure 12 for a circular harbour (see § 6 below) in order to illustrate the contiguous effects of parallel and series resonance in the neighbourhood of parallel resonance (which does *not* occur in the Helmholtz mode).

The limiting form of (3.11) for very long waves, such that $Z_M + Z_H$ is dominated by $Z_0 = 1/(j\omega A)$, is

$$\zeta_s \sim -\tfrac{1}{2} j k^2 A V_i H_0^{(2)}(kr) \quad (k^2 A \to 0). \tag{4.24}$$

This result may be of some interest in connexion with the effects of coastal topography on tidal phases (Munk, private communication).

5. Equivalent circuit for canal

We now interpose a canal† of breadth b and length l between the harbour and the coast, as shown in figure 4, and obtain the equivalent circuit on the assumption that only plane waves need be considered in the canal. This approximation is strictly valid only for $kb \ll 1$, but we show in the appendix that the effects of the cross-waves (y-dependent modes) are not likely to be significant for $kb < \pi$.

Invoking the plane-wave approximation, $u = u(x)$ and $\zeta = \zeta(x)$, in (2.3) and (2.4), we obtain

$$I(x) = bhu(x) \quad \text{and} \quad V(x) = \zeta(x). \tag{5.1a, b}$$

† We use *canal* in the same sense as Lamb (1932, § 169ff.). Some might regard the synonym *channel* as more appropriate in the present context.

Solving (2.7), subject to the assumed values I_1 and I_2 at $x = 0$ and l, respectively, we obtain the transmission-line solution,

$$I(x) = \csc kl[I_1 \sin k(l-x) + I_2 \sin kx] \tag{5.2a}$$

and
$$V(x) = (jbc \sin kl)^{-1}[I_1 \cos k(l-x) - I_2 \cos kx]. \tag{5.2b}$$

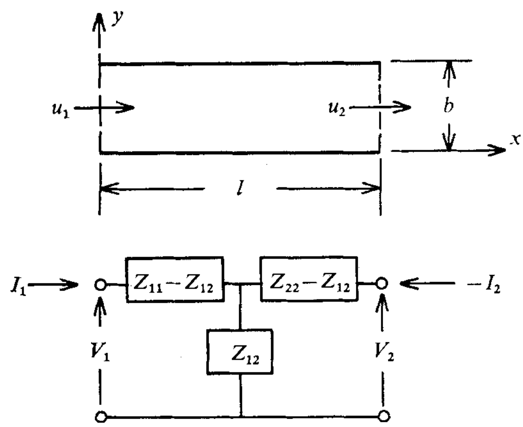

FIGURE 4. Canal and equivalent circuit for the plane-wave approximation. The impedances $Z_{11} = Z_{22}$ and Z_{12} are given by (5.4).

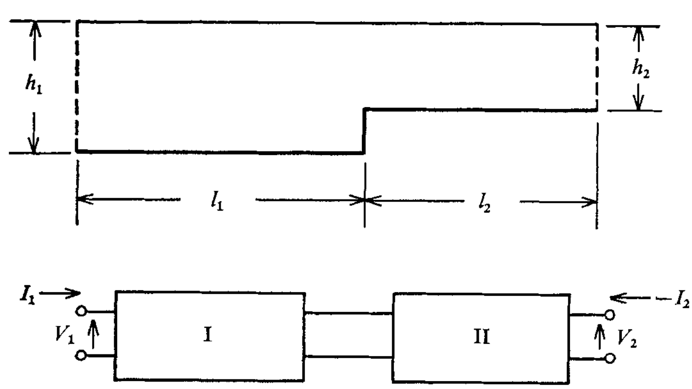

FIGURE 5. The equivalent circuit for a stepped canal. The networks I and II are calculated as in figure 4, using $h = h_1$ and $l = l_1$ in I and $h = h_2$ and $l = l_2$ in II. If the step is in breadth, rather than depth, the impedance $Z(\beta)$, as given by (5.5), must be inserted in the upper connexion between I and II.

Setting $V(0) = V_1$ and $V(l) = V_2$ in (5.2b), we obtain the matrix equation

$$\begin{Bmatrix} V_1 \\ V_2 \end{Bmatrix} = \begin{bmatrix} Z_{11} & Z_{12} \\ Z_{12} & Z_{22} \end{bmatrix} \begin{Bmatrix} I_1 \\ -I_2 \end{Bmatrix}, \tag{5.3}$$

where
$$Z_{11} = Z_{22} = -(j/bc)\cot kl, \quad Z_{12} = -(j/bc)\csc kl,$$

and
$$Z_{11} - Z_{12} = Z_{22} - Z_{12} = (j/bc)\tan \tfrac{1}{2}kl. \tag{5.4}$$

The four-terminal network implied by (5.3) and (5.4) is sketched in figure 4, wherein the arms $(Z_{11} - Z_{12})$ and pillar (Z_{12}) are inductive and capacitative, respectively, for $kl < \pi$ (l less than a half-wavelength).

The preceding results remain valid for a canal of arbitrary (but constant) cross-section S if $h \equiv S/b$, where b is the breadth of the canal at the free surface (Lamb, § 169). The results also are valid for a canal of variable depth in the sense that the effects of the cross-waves (y-dependent modes) that are generated by a change in depth are negligible in the shallow-water approximation (see Lamb (§ 176) for a qualitative argument, and Bartholomeusz (1958) for a proof). The equivalent circuit for a canal of variable depth may be approximated by dividing the canal into segments of constant depth and cascading the four-terminal networks for the individual segments, as illustrated in figure 5. The effect of a

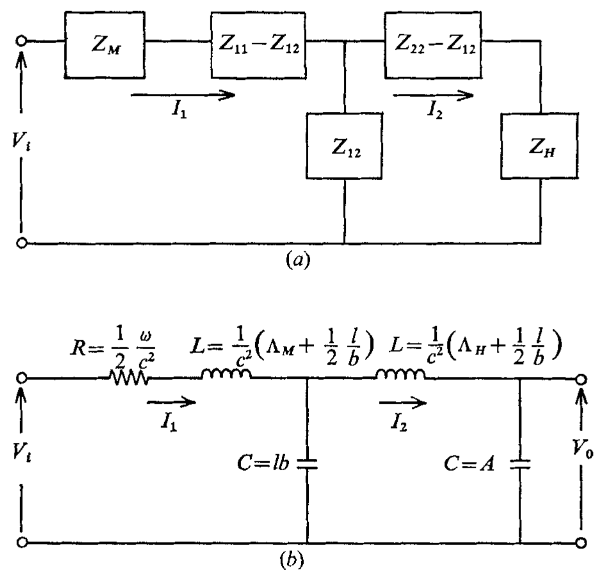

FIGURE 6. Equivalent circuit for harbour connected to coast through canal: (*a*) general case; (*b*) Helmholtz mode ($k^2A \ll 1$, $kl \ll 1$).

change in breadth may be inferred from the corresponding acoustical problem (Miles 1946). Suppose, for example, that the breadth decreases abruptly from b_1 to b_2 in consequence of a step on one side of the canal. The equivalent circuit for the stepped canal then consists of the cascaded, four-terminal networks of figure 5 plus an impedance, $Z(\beta)$, that must be inserted in the upper connexion between I and II. Invoking the approximation $kb_1 \ll 1$, we obtain (Miles 1946; equation (132), wherein $Z(\beta) = (j/b_1c)(B^0/Y^0)$ and $\beta = \alpha$)

$$Z(\beta) = 2(j\omega/\pi c^2)\left[\log\{(1-\beta^2)/(4\beta)\}+\tfrac{1}{2}(\beta+\beta^{-1})\log\{(1+\beta)/(1-\beta)\}\right], \quad (5.5)$$

wherein $\beta \equiv b_2/b_1 < 1$ (b_2 is defined as the breadth of the narrower channel, which may be on either side of the discontinuity).

Inserting the equivalent circuit for the canal between the equivalent circuits for the harbour mouth (at $x = 0$) and the harbour (at $x = l$), we obtain the equivalent circuit shown in figure 6 (*a*). Calculating I_2 and the corresponding voltage drop across Z_n and invoking (4.3*a*) for the modal amplification factor, we obtain

$$\mu_n^{\frac{1}{2}}\mathscr{A}_n(\kappa) = |V_i|^{-1}\,|Z_nI_2| \quad (5.6a)$$

$$= |(Z_M+Z_{11})(Z_H+Z_{22})-Z_{12}^2|^{-1}\,|Z_nZ_{12}| \quad (5.6b)$$

$$= |(Z_M+Z_H)\cos kl + j\{(bc)^{-1}+bcZ_MZ_H\}\sin kl|^{-1}\,|Z_n|, \quad (5.6c)$$

where (5.6c) follows from (5.6b) through (5.4). The frequency dependence of $\mathscr{A}_n(\kappa)$ is qualitatively similar to that established in § 4, but $\tilde{\kappa}_n - \kappa_n$ may not be small. The values of $\tilde{\mathscr{A}}_n$ and Q_n may be substantially larger than those given by (4.10) and (4.13); however, (4.18) remains valid for $n \neq 0$, and the results therefore are of limited interest. There also exist modes that correspond to resonance of the canal itself, for which $x = l$ is approximately a node and the motion excited in H is small, but these, too, are governed by (4.18), in the sense that decreasing the channel width does not affect the mean response of the canal to a random input except in the Helmholtz mode.

We consider further the special case of Helmholtz resonance, assuming $kl \ll 1$ as well as $k^2A \ll 1$. The equivalent circuit then reduces to that of figure 6 (b). Calculating $|V_0/V_i|$ in this circuit, and neglecting terms of $O(k^2bl)$ relative to unity, we obtain

$$\mathscr{A}_0(\kappa) = \{\tfrac{1}{4}(1+\alpha)^2\kappa^2 + [\kappa\Lambda(\kappa) - 1]^2\}^{-\frac{1}{2}}, \tag{5.7}$$

where

$$\alpha = bl/A \tag{5.8}$$

is the ratio of the canal and harbour areas, and

$$\Lambda(\kappa) = \Lambda_H^{(0)} + (1+\alpha)\,\Lambda_M(ka) + (1+\tfrac{1}{2}\alpha)\,(l/b). \tag{5.9}$$

Resonance is determined by $\tilde{\kappa}_0\Lambda(\tilde{\kappa}_0) = 1$, and yields

$$\tilde{\mathscr{A}}_0 = Q_0 = 2(1+\alpha)^{-1}\tilde{\kappa}_0^{-1} \tag{5.10}$$

and

$$\mathscr{P}_0 = \tfrac{1}{2}(1+\alpha)^{-1}\tilde{\kappa}_0^{-\frac{1}{2}} \tag{5.11}$$

in place of (4.10a), (4.13a), and (4.18). The resonance curve of (5.7) is illustrated in figure 10, using the results of the following section.

6. Circular harbour

The eigenfunctions determined by (2.10) for a circular harbour of radius R are given by

$$\psi_{0s}(r,\theta) = A^{-\frac{1}{2}}[J_0(j'_{0s})]^{-1} J_0(j'_{0s}r/R) \quad (m = 0), \tag{6.1a}$$

$$\psi_{ms}(r,\theta) = \left(\frac{2}{A}\right)^{\frac{1}{2}}\left[1-\left(\frac{m}{j'_{ms}}\right)^2\right]^{-\frac{1}{2}} \frac{J_m(j'_{ms}r/R)}{J_m(j'_{ms})}\begin{Bmatrix}\cos m\theta\\ \sin m\theta\end{Bmatrix} \quad (m \geqslant 1), \tag{6.1b}$$

and

$$J'_m(j'_{ms}) = 0 \quad (m = 0,1,2,\ldots;\ s = 0,1,2,\ldots), \tag{6.1c}$$

where r is the polar radius measured from the centre of the harbour, θ is the polar angle measured from the mid-plane of the mouth, we write $\psi_{ms}(r,\theta)$ in place of $\psi_n(x,y)$, the indices m (the number of azimuthal modes) and s (the number of radial nodes) jointly replace the single index n in § 2, and the eigenfunctions obtained by choosing the alternatives $\cos m\theta$ and $\sin m\theta$ are distinct. The eigenvalues are given by

$$\kappa_{ms} = \pi(j'_{ms})^2. \tag{6.2}$$

The zeroth mode of (2.11) corresponds to $m = s = 0$, for which $j'_{00} \equiv 0$.

We specify M by $R = 1$ and $-\tfrac{1}{2}\theta_M < \theta < \tfrac{1}{2}\theta_M$, where

$$\theta_M \equiv a/R \ll 1, \tag{6.3}$$

by virtue of which we may neglect the curvature of the harbour boundary over its intersection with the straight coastline. The essential approximation is $\sin\frac{1}{2}\theta_M \doteqdot \frac{1}{2}\theta_M$, which is in error by less than 5% for $a/R < 1$.

Substituting (6.1) and (3.6) into (2.17), we obtain

$$\mu_{ms} = (2-\delta_{0m})\,[1-(m/j'_{ms})^2]^{-1}\,[1+O(m^2\theta_M^2)] \tag{6.4}$$

for the $\cos m\theta$ modes and $\mu_{ms} = 0$ for the $\sin m\theta$ modes. The approximation (6.4) is not uniformly valid as $m \to \infty$, but it suffices for all but the calculation of $\Lambda_H^{(0)}$ through (2.20b). The result for the $\sin m\theta$ modes follows from the assumption that $f(y)$ is an even function of y, which is strictly true only for normal incidence; however, the contribution of these modes to Λ_H is small relative to the contribution of the $\cos m\theta$ modes.

Substituting $\psi_{ms}(R,\theta)\,\psi_{ms}(R,\phi)$ from (6.1) for $\psi_n(0,y)\,\psi_n(0,\eta)$ in (2.19b) and replacing the summation over n by a double summation over m and s (excluding the term for $m = s = 0$), we obtain

$$\pi G^{(0)}(y,\eta) = \pi \sum_{m=0}^{\infty}\sum_{s=0}^{\infty} k_{ms}^{-2}\psi_{ms}(R,\theta)\,\psi_{ms}(R,\phi) \tag{6.5a}$$

$$= \sum_{s=1}^{\infty}(j'_{0s})^{-2} + 2\sum_{m=1}^{\infty}\sum_{s=0}^{\infty}[(j'_{ms})^2-m^2]^{-1}\cos m(\theta-\phi) \tag{6.5b}$$

$$= \tfrac{1}{8} + \sum_{m=1}^{\infty} m^{-1}\cos m(\theta-\phi) \tag{6.5c}$$

$$= \tfrac{1}{8} - \log\,[2\sin(\tfrac{1}{2}|\theta-\phi|)] \tag{6.5d}$$

$$= \tfrac{1}{8} - \log(|y-\eta|/R) \quad (|\theta,\phi| \ll 1), \tag{6.5e}$$

where (6.5c) follows from (6.5b) with the aid of the partial-fraction expansion of $J_m(x)/xJ'_m(x)$ in the limit $x \to 0$ (or alternatively, from the solution of (2.22) as $k \to 0$). Substituting (6.5e) into (2.20a) and invoking the approximation (3.6) for $f(y)$, we obtain

$$\pi\Lambda_H^{(0)} = \tfrac{1}{8} + \ln(4R/a) \quad (\theta_M \ll 1). \tag{6.6}$$

Combining (3.9) and (6.6) in (4.7), and invoking (4.8b) for $n \neq 0$, we obtain

$$\pi\Lambda_{ms} = 3{\cdot}0135 + 2\ln(R/a) - \ln(kR), \tag{6.7}$$

wherein $k = k_{ms}$ for $n \neq 0$.

Substituting (6.4) and (6.7) into (4.9) and invoking (4.8b) for $n \neq 0$, we obtain the series-resonant wave-numbers,

$$\tilde{k}_{ms}R \equiv (\tilde{\kappa}_{ms}/\pi)^{\frac{1}{2}}, \tag{6.8}$$

tabulated in table 1. The preceding approximations appear to be reasonable for $a/R \leqslant 0{\cdot}3$. The results for $0{\cdot}3 < a/R \leqslant 1{\cdot}0$ are included for rough comparison.

We illustrate the coupling between relatively well separated modes, $\epsilon \gg 1$ in (4.20), by invoking (4.19) in place of (4.5) for the Helmholtz and (1, 0) modes ($\kappa_n \to 0$ and $\kappa_m \to \kappa_{10}$ in (4.19) and (4.20)). Retaining only the dominant terms, as in (4.7a) and (4.8b), we obtain

$$\tilde{\kappa}^{-1} = \mu_{10}(\tilde{\kappa}-\kappa_{10}) = \Lambda_H^{(0)} + \Lambda_M(ka) \tag{6.9}$$

in place of (4.9). The two roots of (6.9) are tabulated in the third and fourth columns of table 1 between the corresponding, single-mode approximations. The relative change in $\tilde{k}_{00}$ is negligible, and that in $\tilde{k}_{10}$ less than 2 %, for $a/R \leqslant 0{\cdot}3$; however, the relative change in $\tilde{k}_{10} - k_{10}$ is significant.

The (4, 0) and (1, 1) modes have nearly equal eigenvalues, for which $\epsilon \ll 1$ in (4.20). The corresponding series-resonant wave-number given by (4.21) is

		$\tilde{k}_{ms}R$							
a/R \ (m, s)	(0, 0)	(0, 0) and (1, 0)	(1, 0)	(2, 0)	(0, 1)	(3, 0)	(4, 0)	(4, 0) and (1, 1)	(1, 1)
0	0	0 1·841	1·841	3·054	3·832	4·201	5·318	5·322	5·331
0·01	0·272	0·272, 1·913	1·907	3·106	3·844	4·246	5·359	5·381	5·349
0·03	0·298	0·298, 1·932	1·923	3·118	3·847	4·258	5·370	5·397	5·354
0·1	0·339	0·338, 1·968	1·951	3·142	3·853	4·280	5·391	5·426	5·364
0·3	0·397	0·396, 2·042	2·001	3·187	3·864	4·323	5·433	5·487	5·383
1·0	0·522	0·517, 2·434	2·162	3·356	3·910	4·509	5·641	5·771	5·476

TABLE 1. The series-resonant wave-numbers, $\tilde{k}_{ms}R$, for a circular harbour. The results are based on the single-mode approximation of (4.9) except as noted. The third and fourth, and the ninth, columns illustrate the effects of coupling between well separated and nearly degenerate modes, respectively.

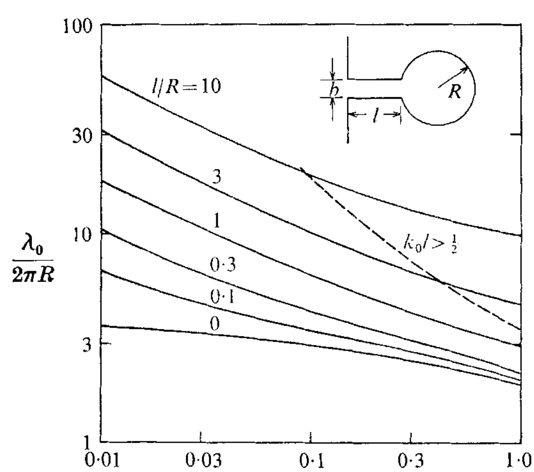

b/R

FIGURE 7

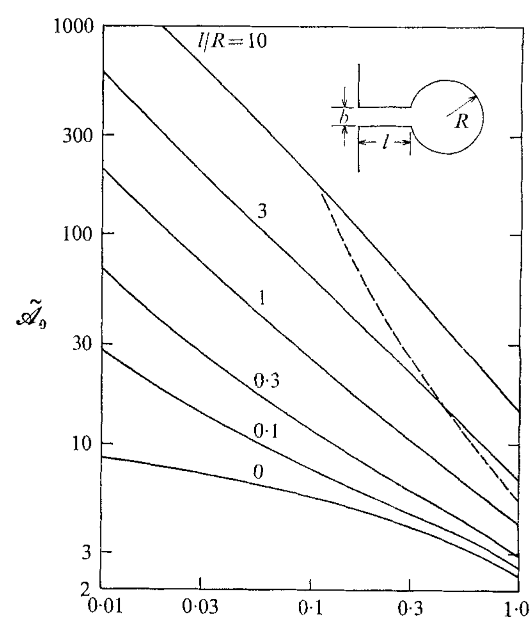

b/R

FIGURE 8

FIGURE 7. Wavelength for Helmholtz resonance of circular harbour plus canal ($b \equiv a$ for $l = 0$). The results are strictly valid only for $b/R \ll 1$ and $k_0 l \ll 1$, but the corresponding errors are not likely to exceed 5–10 % for $b/R < 1$ and $k_0 l < \frac{1}{2}$.

FIGURE 8. Resonant amplification factor, $\tilde{\mathscr{A}}_0 = Q_0$, for Helmholtz mode in circular harbour. $k_0 l > \frac{1}{2}$ to the right of the dashed line.

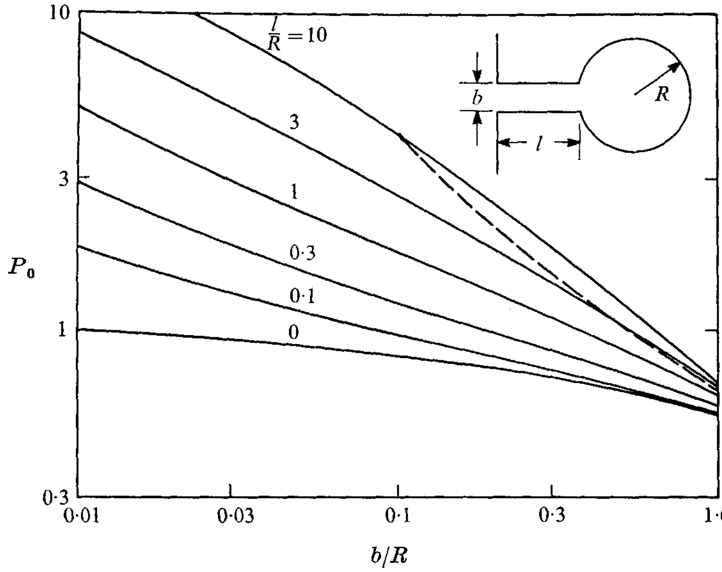

FIGURE 9. Power-spectrum amplification factor for Helmholtz mode in circular harbour. $k_0 l > \frac{1}{2}$ to the right of the dashed line.

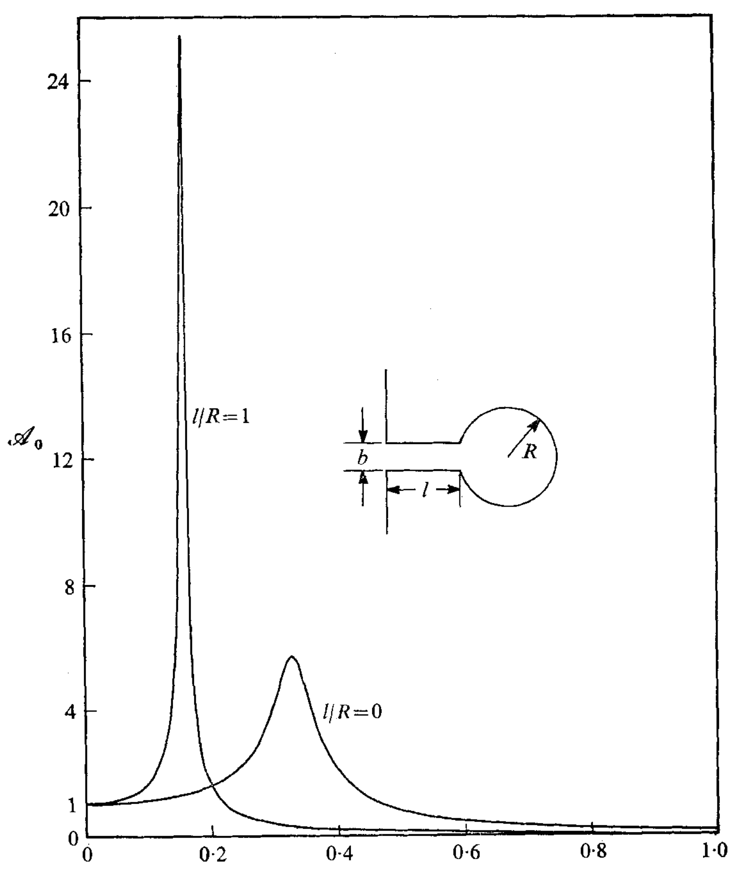

FIGURE 10. Resonance curve for Helmholtz mode in circular harbour, as given by (5.7) and (6.7) for $a/R = 0{\cdot}1$ ($b \equiv a$).

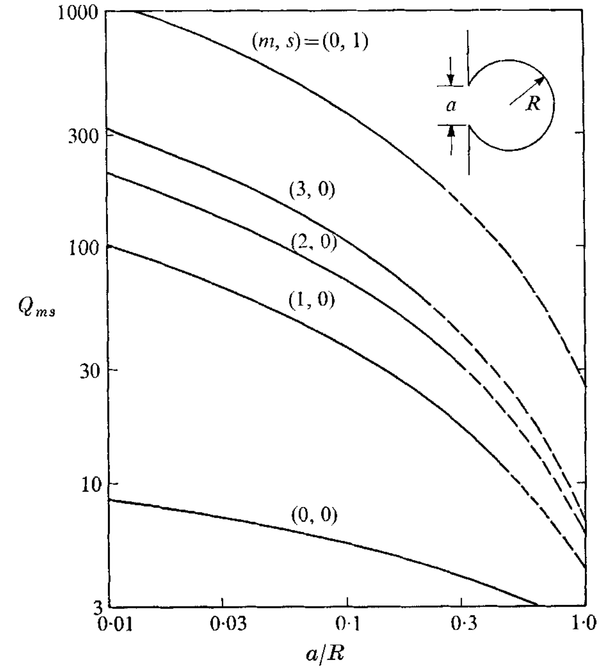

FIGURE 11. Q_{ms} for the first five modes in a circular harbour. The dashed portions of the curves correspond to $ka > 1$.

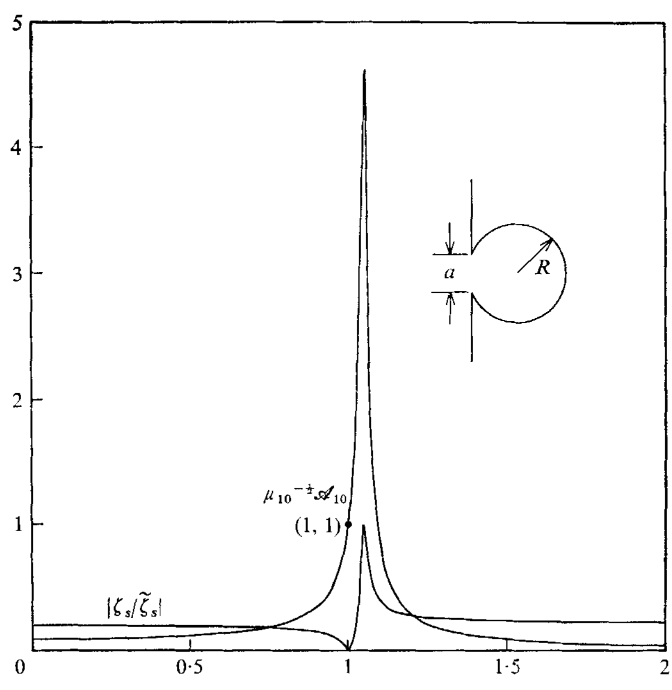

FIGURE 12. Resonance curve for 10 mode ($k_{10}R = 1{\cdot}841$) in circular harbour. The amplification factor is given by (4.6a) and (6.7), whilst the scattering-amplitude ratio is based on (4.23b) and (6.7).

tabulated in the ninth column of table 1 and is seen to be larger than (the single-mode approximations to) both $\tilde{\kappa}_{40}$ and $\tilde{\kappa}_{11}$, although the relative changes are less than 1 % and 2 %, respectively, for $a/R \leqslant 0{\cdot}3$ (but, as in the preceding example, the relative changes in $\tilde{k}-k_{40}$ and $\tilde{k}-k_{11}$ are significant).

The resonant wavelength, $\lambda_0 = 2\pi/\tilde{k}_0$, $\tilde{\mathscr{A}}_0 = Q_0$, and $\mathscr{P}_0$ for the Helmholtz mode, as determined by (4.9*a*), (4.10*a*), (4.13*a*), and (4.18) in conjunction with (6.7) are given by the lowest curves in each of figures 7–9. The higher curves in figures 7–9 are based on (5.7)–(5.11) and illustrate the striking effects of an intervening canal on Helmholtz resonance. Typical resonance curves for the Helmholtz mode are plotted in figure 10. Q_{ms}, as determined by (4.13), is plotted in figure 11 for the first five modes. The resonance curve for the 10 mode is plotted in figure 12. The remarkable sharpness of the higher modes, *vis-à-vis* the Helmholtz mode (in the absence of a canal), is borne out by Lee's (1971) experiments.

The period for the Helmholtz mode is given by

$$T_0 = \lambda_0/c = 2\pi(A/gh)^{\frac{1}{2}}\tilde{\kappa}_0^{\frac{1}{2}}. \tag{6.10}$$

Choosing $R = 1000'$ and $h = 20'$, we obtain $T_0 = 2\lambda_0/\pi R$ minutes, which approximates typical tsunami periods (20–40 min) for $\lambda_0/2\pi R$ in the range of 5–10 (see figure 7). We infer that a large harbour with a short entrance ($l/R \ll 1$), or a small harbour with a canal ($l/R \sim 0{\cdot}3$–3), may act as a Helmholtz resonator under tsunami excitation.

7. Rectangular harbour

The eigenfunctions and eigenvalues determined by (2.10) for a rectangular harbour bounded by $x = 0, X$ and $y = 0, Y$ (so that the origin for x and y now is placed at one corner of the harbour) are given by

$$\psi_{mn} = \left(\frac{2-\delta_{0m}}{X}\right)^{\frac{1}{2}}\left(\frac{2-\delta_{0n}}{Y}\right)^{\frac{1}{2}}\cos\left(\frac{m\pi x}{X}\right)\cos\left(\frac{n\pi y}{Y}\right) \tag{7.1}$$

and $$k_{mn}^2 = (m\pi/X)^2+(n\pi/Y)^2 \quad (m = 0,1,2,\ldots;\ n = 0,1,2,\ldots), \tag{7.2}$$

where the joint indices m and n replace n in § 2, and the zeroth mode of (2.11) corresponds to $m = n = 0$.

Substituting (7.1) and (7.2) into (2.19*b*), we obtain

$$G^{(0)}(y,\eta) = \frac{2}{XY}\left\{\sum_{m=1}^{\infty}\left(\frac{X}{m\pi}\right)^2 + \sum_{m=0}^{\infty}\sum_{n=1}^{\infty}\frac{(2-\delta_{0m})\cos(n\pi y/Y)\cos(n\pi\eta/Y)}{(m\pi/X)^2+(n\pi/Y)^2}\right\} \tag{7.3a}$$

$$= \frac{1}{3}\left(\frac{X}{Y}\right)+\frac{2}{\pi}\sum_{n=1}^{\infty}\frac{1}{n}\coth\left(\frac{n\pi X}{Y}\right)\cos\left(\frac{n\pi y}{Y}\right)\cos\left(\frac{n\pi\eta}{Y}\right) \tag{7.3b}$$

$$= \frac{1}{3}\left(\frac{X}{Y}\right)-\frac{1}{\pi}\log\left\{2\left|\cos\left(\frac{\pi y}{Y}\right)-\cos\left(\frac{\pi\eta}{Y}\right)\right|\right\}$$
$$+\frac{2}{\pi}\sum_{n=1}^{\infty}\frac{1}{n}\left[\coth\left(\frac{n\pi X}{Y}\right)-1\right]\cos\left(\frac{n\pi y}{Y}\right)\cos\left(\frac{n\pi\eta}{Y}\right), \tag{7.3c}$$

where (7.3*b*) follows from (7.3*a*) with the aid of the partial-fraction expansion of the hyperbolic co-tangent. The series in (7.3*b*) may be summed without further approximation, but the result (which may be obtained by solving the corresponding problem in potential theory) involves elliptic functions. The error in neglecting the series in (7.3c) is less than 10% (0·5%) for $X/Y > \frac{1}{4}$ ($\frac{1}{2}$).

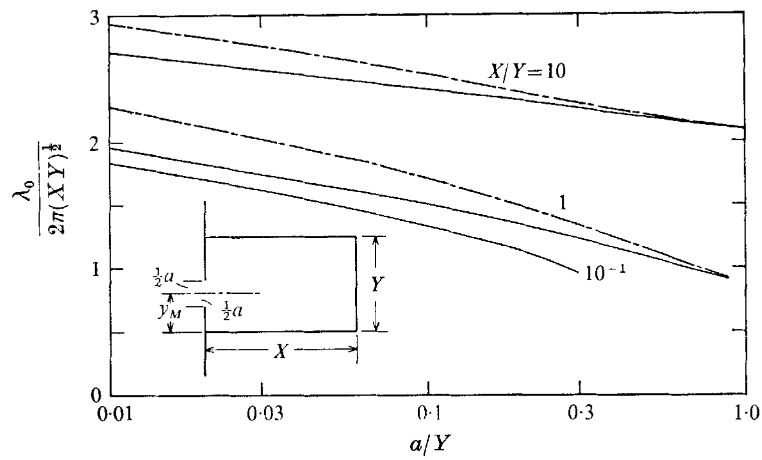

FIGURE 13. Wavelength for Helmholtz resonance of rectangular harbour with entrance at either one end ($y_M = \frac{1}{2}a$, — · —) or centre ($y_M = \frac{1}{2}Y$, ——). The lower curves have been terminated on the right at $ka = 1$.

Turning to the estimation of $\Lambda_H^{(0)}$, we specify M by $x = 0$ and $y = y_M \pm \frac{1}{2}a$, introduce the change of variable

$$\cos(\pi y/Y) = \cos\alpha\cos\beta + \sin\alpha\sin\beta\cos\phi \quad (\alpha = \pi a/2Y, \beta = \pi y_M/Y), \tag{7.4}$$

which maps M on $0 < \phi < \pi$, and pose the trial function in the form

$$f(y)\,dy = d\phi/\pi, \tag{7.5}$$

which is equivalent to (3.5) for $a/Y \to 1$ and to (3.6) for $a/Y \to 0$. Substituting (7.3c), (7.4) and (7.5) into (2.20a), we obtain

$$\pi\Lambda_H^{(0)} = \tfrac{1}{3}\pi(X/Y) + \log(\csc\alpha\csc\beta) + \sum_{n=1}^{\infty} n^{-1}\mu_{0n}[\coth(n\pi X/Y) - 1] \tag{7.6a}$$

$$= \tfrac{1}{3}\pi(X/Y) + \log(\csc\alpha\csc\beta) + 4\exp(-2\pi X/Y)\cos^2\alpha\cos^2\beta + O\{\exp(-4\pi X/Y)\}, \tag{7.6b}$$

where μ_{0n} is given by (7.7) below, and (7.6b) follows from (7.6a) through the expansion of $\coth(n\pi X/Y)$ in powers of $\exp(-2\pi X/Y)$.

Substituting (7.1), (7.4), and (7.5) into (2.17), we obtain

$$\mu_{mn} = (2-\delta_{0m})(2-\delta_{0n})\left\{(1/\pi)\int_0^{\pi}\cos(n\pi y/Y)\,d\phi\right\}^2 \tag{7.7a}$$

$$= 2-\delta_{0m} \quad (n=0) \tag{7.7b}$$

$$= 2(2-\delta_{0m})\cos^2\alpha\cos^2\beta \quad (n=1) \tag{7.7c}$$

$$= 2(2-\delta_{0m})(3\cos^2\alpha\cos^2\beta - \cos^2\alpha - \cos^2\beta)^2 \quad (n=2) \tag{7.7d}$$

$$= (2-\delta_{0m})(2-\delta_{0n})\cos^2 n\beta[1+O(\alpha^2)] \quad (\alpha \to 0). \tag{7.7e}$$

The Helmholtz-resonance parameter, $\tilde{\kappa}_0^{-\frac{1}{2}} = \lambda_0/(2\pi A^{\frac{1}{2}})$, as determined by (4.9$a$) in conjunction with (4.7a) and (7.6a), is plotted in figures 13 and 14. The corresponding values of $\tilde{\mathscr{A}}_0$ and Q_0 are determined by (4.13a). The results for a square harbour with centred entrance ($X = Y$ and $y_m = \frac{1}{2}Y$) differ from those of a

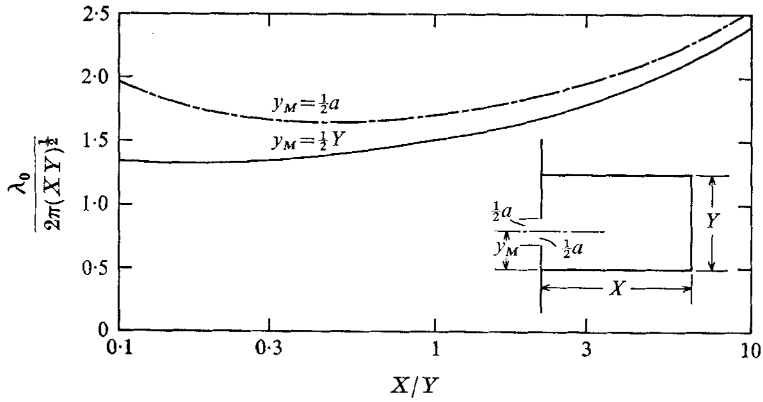

FIGURE 14. Wavelength for Helmholtz resonance of rectangular harbour with entrance at either one end ($y_M = \frac{1}{2}a$, — - —) or centre ($y_M = \frac{1}{2}Y$, ——).

$(m, n) =$		0, 1	0, 2	1, 0	1, 1	1, 2	2, 0	2, 1	2, 2
a/Y	X/Y				$y_M = \frac{1}{2}Y$				
10^{-2}	$\frac{1}{2}$	—	160	160	—	148	545	—	332
	1	—	359	103	—	219	359	—	333
	2	—	885	709	—	468	251	—	542
10^{-1}	$\frac{1}{2}$	—	39·8	37·8	—	33·7	107	—	66·0
	1	—	99·7	30·9	—	59·5	94·8	—	86·0
	2	—	294	267	—	155	87·4	—	177
					$y_M = \frac{1}{2}a$				
10^{-2}	$\frac{1}{2}$	97·7	354	353	217	335	1270	671	780
	1	205	745	205	195	458	743	457	707
	2	472	1725	129	291	913	472	451	1062
10^{-1}	$\frac{1}{2}$	263	99·5	81·3	51·5	89·0	258	143	190
	1	57·9	222	55·1	52·6	134	181	115	200
	2	151	591	41·9	91·6	312	143	139	359

TABLE 2. Q_{ms} for rectangular harbour.

circular harbour of the same area and $a/R = 2y_m/Y$ by less than 1 %. Introducing a canal increases $\tilde{\kappa}_0^{-\frac{1}{2}}$ to values comparable with those of figure 7 (note that $\lambda_0/2\pi R = \pi^{\frac{1}{2}}\tilde{\kappa}_0^{-\frac{1}{2}}$ in figure 7).

The calculations for the higher modes are straightforward but form a five-parameter $(m, n, a/Y, y_m/Y, X/Y)$ family. We list representative values of Q_{mn}, as determined by (4.13b) in conjunction with (4.8a), (7.2), (7.6a), and (7.7), in table 2. These values are comparable with those for the higher modes in the circular harbour.

Appendix. Cross-waves in canal

The plane-wave approximation is violated, and the results of § 5 require modification, in the neighbourhoods of discontinuities such as those at the seaward and harbour ends of the canal in figure 4. The exact solution of (2.7) in the rectangular canal extending from $x = 0$ to $x = l$ and bounded by $y = 0, b$ is given by (2.8), extended to include the excitation at both ends of the canal:

$$\zeta(x,y) = (j\omega/g)\int_0^b [G(x,y;0,\eta)\,u(0,\eta) - G(x,y;l,\eta)\,u(l,\eta)]\,d\eta, \qquad \text{(A 1)}$$

where G is the Green's function for the rectangular harbour (with $X = l$ and $Y = b$), and the opposing signs of the terms at the two ends of the canal reflect the fact that the normals to the end planes at $x = 0$ and l are oppositely directed. An alternative representation of the Green's function, which proves more convenient in the present context than the normal-mode representation implied by (2.9) and (7.1, 2), is given by

$$G(x,y;\xi,\eta) = -(kb)^{-1}\csc kl\cos[k(l-|x-\xi|)] + \mathscr{G}(l-|x-\xi|,y,\eta), \qquad \text{(A 2)}$$

where $$\mathscr{G}(x,y,\eta) = \frac{2}{b}\sum_{n=1}^{\infty}\frac{\cosh(\kappa_n x)}{\kappa_n \sinh(\kappa_n l)}\cos\left(\frac{n\pi y}{b}\right)\cos\left(\frac{n\pi\eta}{b}\right), \qquad \text{(A 3)}$$

and $$\kappa_n = [(n\pi/b)^2 - k^2]^{\frac{1}{2}}. \qquad \text{(A 4)}$$

Substituting (A 2),

$$u(0,y) = (I_1/h)f_1(y), \quad \text{and} \quad u(l,y) = (I_2/h)f_2(y) \qquad \text{(A 5)}$$

into (A 1) and invoking the normalization of (2.12b) for f_1 and f_2, we obtain

$$\zeta(x,y) = \zeta^{(0)} + (j\omega/c^2)\left[I_1\int_0^b \mathscr{G}(l-x,y,\eta)f_1(\eta)\,d\eta - I_2\int_0^b \mathscr{G}(x,y,\eta)f_2(\eta)\,d\eta\right], \qquad \text{(A 6)}$$

where $\zeta^{(0)}$, the plane-wave solution, is given by (5.2b). Substituting (A 6) into (2.13) and placing the results for V_1 ($x = 0$) and V_2 ($x = l$) in the form (5.3), we obtain

$$Z_{rs} = Z_{rs}^{(0)} + (j\omega/c^2)\int_0^b\int_0^b \mathscr{G}(\delta_{rs}l,y,\eta)f_r^*(y)f_s(\eta)\,d\eta\,dy \quad (r = 1,2;\ s = 1,2), \qquad \text{(A 7)}$$

where $Z_{rs}^{(0)}$ is given by (5.4), and δ_{rs} is the Kronecker delta.

The contributions of the cross-waves, as represented by the second terms on the right-hand sides of both (A 6) and (A 7), vanish identically in the plane-wave approximation, which implies $f_1(y) = f_2(y) = 1/b$. These contributions will be finite but small for any other reasonable approximations to $f_{1,2}$ if $kb < \pi$. We consider, e.g. (cf. (3.6)),

$$f_1(y) = f_2(y) = \pi^{-1}y^{-\frac{1}{2}}(b-y)^{-\frac{1}{2}} \equiv f(y), \qquad \text{(A 8)}$$

which is likely to overestimate the cross-wave contributions in consequence of overestimating the strength of the singularities at $y = 0$ and $y = b$ (the actual singularity for a rectangular corner at $y = 0$ must be like $y^{-\frac{1}{3}}$, rather than $y^{-\frac{1}{2}}$). Substituting (A 3) into (A 7), and invoking (A 8) and the corresponding integral

$$\int_0^b \cos(n\pi y/b)f(y)\,dy = J_0(\tfrac{1}{2}n\pi)\cos(\tfrac{1}{2}n\pi), \qquad \text{(A 9)}$$

which vanishes for n odd, we obtain (with $n = 2m$)

$$Z_{rs} - Z_{rs}^{(0)} = \frac{2j\omega}{bc^2} \sum_{m=1}^{\infty} \frac{\cosh(\delta_{rs} k_{2m} l)}{k_{2m} \sinh(k_{2m} l)} J_0^2(m\pi) \tag{A 10a}$$

$$\doteqdot \frac{2j\omega}{\pi^2 bc^2} \sum_{m=1}^{\infty} \frac{\cosh(\delta_{rs} k_{2m} l)}{m k_{2m} \sinh(k_{2m} l)} \tag{A 10b}$$

$$\doteqdot \frac{j\omega}{\pi^3 c^2} \sum_{m=1}^{\infty} \frac{\cosh(2\delta_{rs} m\pi l/b)}{m^2 \sinh(2m\pi l/b)} \quad (kb \ll 2\pi) \tag{A 10c}$$

$$= (j\omega/\pi c^2)\left[\tfrac{1}{6}\delta_{rs} + O\{\exp(-2\pi l/b)\}\right], \tag{A 10d}$$

where (A 10b) follows from (A 10a) after invoking the asymptotic approximation to $J_0(m\pi)$, which introduces an error of less than 5%, and (A 10c) follows from (A 10b) after invoking the approximation $k_n = n\pi/b$. The approximation (A 10d) is adequate for $kb < \pi$ and $l > b$ and implies that $Z_{rs} - Z_{rs}^{(0)}$ is not likely to be significant *vis-à-vis* either $Z_{rs}^{(0)}$ or Z_M. It is true that $Z_{rs} - Z_{rs}^{(0)}$ achieves large values as $l/b \to 0$, but then it is only of the order of $10^{-2}(kb)^2 Z_{rs}^{(0)}$ and introduces less than a 10% error (for $kb < \pi$); moreover, the effects of the canal vanish with l/b.

REFERENCES

BARTHOLOMEUSZ, E. F. 1958 The reflexion of long waves at a step. *Proc. Camb. Phil. Soc.* **54**, 106–18.

CARRIER, G. F., SHAW, R. P. & MIYATA, M. 1970 The response of narrow mouthed harbors in a straight coastline to periodic incident waves. *J. Appl. Mech.* (in the press).

GARRETT, C. J. R. 1970 Bottomless harbours. *J. Fluid Mech.* **43**, 433–49.

HWANG, L. S. & TUCK, E. O. 1970 On the oscillations of harbours of arbitrary shape. *J. Fluid Mech.* **42**, 447–64.

LAMB, H. 1932 *Hydrodynamics*. Cambridge University Press.

LEE, J. J. 1971 Wave induced oscillations in harbours of arbitrary geometry. *J. Fluid Mech.* **45**, 375–93.

MILES, J. W. 1946 The analysis of plane discontinuities in cylindrical tubes. Parts I and II. *J. Acoust. Soc. Am.* **17**, 259–71, 272–84.

MILES, J. W. 1948 The coupling of a cylindrical tube to a half-infinite space. *J. Acoust. Soc. Am.* **20**, 652–64.

MILES, J. W. 1967 Surface-wave scattering matrix for a shelf. *J. Fluid Mech.* **28**, 755–67.

MILES, J. W. & MUNK, W. H. 1961 Harbor paradox. *J. Waterways Harb. Div., Am. Soc. Civ. Engrs* **87**, 111–30.

MORSE, P. M. 1948 *Vibration and Sound*. McGraw-Hill.

RAYLEIGH, LORD 1945 *Theory of Sound*. Dover.

SOMMERFELD, A. 1949 *Partial Differential Equations in Physics*. Academic.